Pattern Recognition Letters, *December 2015*

Recovering and Matching Minutiae Patterns from Finger Knuckle Images

Ajay Kumar, *Bichai Wang*
Department of Computing, The Hong Kong Polytechnic University
Hung Hom, Kowloon, Hong Kong

Abstract: *Personal identification approaches using finger knuckle patterns are receiving increasing attention in the biometrics literature. Several approaches have been explored and these methods consider knuckle patterns as textured-like patterns, similar to the iris, and illustrate promising results. However much of the law-enforcement and forensic analysis for hand biometrics still relies on recovery and matching of minutiae patterns which has matured in last several decades. This is largely due to the fact that the identification of minutiae patterns is believed to be more scientific and pervasive in connecting with the anatomy/uniqueness of individuals. Availability of high resolution finger dorsal images acquired for recreational or covert imaging can provide important cues for forensic investigation and analysis, especially when finger dorsal patterns are only the piece of evidence available for the identification. Identification of finger knuckle patterns using minutiae recovery and matching is expected to significantly help in prosecution of such suspects. This paper therefore investigates recovery and matching of minutiae patterns using finger knuckle images. We investigate effective use of minutiae quality in improving performance for the knuckle pattern matching. Our study detailed in this paper also presents comparative evaluation of performance using three popular minutiae matching approaches. The experimental results presented in this paper from a database from 120 different subjects are highly encouraging and validate such first attempt to study minutiae recovery and matching from finger knuckle images.*

1. Introduction

Automated identification of humans using their unique anatomical characteristics has been increasingly investigated for their applications in human surveillance and image forensics. Human fingers are visualized as a complex 3D textured surface consisting of ridges patterns, wrinkles and lines which have been anatomically related to the uniqueness of respective individuals. Finger dorsal patterns are more easily visible from

the individuals hand while they are engaged in a variety of day-to-day activities like writing or signing with a pen, driving a car, playing variety of sports, holding smartphones to firearms. Therefore biometric identification using such finger dorsal imaging has great potential in forensics and surveillance while this biometric has not yet been fully explored. The skin surface on finger dorsal surface joining proximal phalanx and middle phalanx bones is referred to as finger knuckle biometric and is believed to be quite distinctive among individuals. Finger dorsal/knuckle images can also be simultaneously acquired using a low-cost camera while imaging fingerprints, finger-vein, or palmprints and can significantly contribute to the deployment of a more secure and/or convenient multibiometrics system.

Recent report [1] from National Research Council calls for the design and development of forensic science approaches which are more scientific. Law enforcement and forensic experts highly prefer identification of suspects using scientific techniques that are based on quantitative measurements, representative database and statistical models [3]. Such techniques are easy to replicate, more transparent and can be more easily subjected to the validity and reliability evaluations. This is the key reason for preference and successful use of minutiae recovery and matching techniques for the prosecution of suspects using match from their fingerprint images. Finger dorsal images

(a) (b) (c)

Figure 1: Samples depicting knuckle patterns from the images available during day-to-day activities like (a) using smartphones, (b) during sports or (c) functions.

reveal knuckle patterns that are increasingly explored and employed for the identification of suspects [7]. However, to the best of our knowledge, there has not been any study to explore finger knuckle identification using recovery and matching of minutiae patterns. This paper therefore presents a detailed study on completely automated recovery and matching of minutiae patterns using finger knuckle patterns.

1.1 Motivation and Related Work

Finger dorsal images have been increasingly investigated for their use in personal identification and image forensics. There are earlier references in [17] and [2] that demonstrated the promising use of 2D and 3D dorsal patterns respectively for the automated personal identification. Several references explored the effectiveness of such major knuckle texture patterns using texture analysis methods which have shown their effectiveness for well-established biometric modalities like iris, palm or face. Palm dorsal images provide hand geometry details which can be simultaneously acquired and employed [8] to improve the accuracy of knuckle patterns. The experimental results illustrated in the literature from finger dorsal images acquired using constrained imaging [17]-[18], contactless imaging [19] and contactless imaging using mobile phone [20] provide strong motivation for further research in using knuckle patterns as a biometric. Finger dorsal images also illustrate minor knuckle patterns that can be employed [22] for personal identification and also used to improve the accuracy of performance that can be obtained from the simultaneously extracted major knuckle patterns. Reference [16] provides study on stability on knuckle patterns and presents images from over 6 year interval to argue stability of such patterns in various age groups.

Almost all the fingerprint systems employed for the law-enforcement utilize recovery and matching of matching points in fingerprint images. Minutiae based techniques are considered to be more reliable, linked to anatomy of individuals, and successfully

employed for suspect identification during courtroom arguments. The finger knuckle patterns typically illustrate curved lines of varying thickness which (unlike fingerprint ridges) are easily visible from the naked eyes at some distance. These curved lines do intersect with similar curves or lines having varying thickness and generate singularities. The singularities in finger knuckle patterns are quite similar to those observed in fingerprints and their relative location can be used to generate feature templates similar to those employed in fingerprints. There has not been any effort to recover and match minutiae patterns from knuckle images. In view of popularity of minutiae based matching for the fingerprints, success of minutiae based matching of finger knuckle patterns can also provide scientific basis for legal arguments in courtrooms and is investigated in this paper.

The contributions from this paper can be summarized as follows. Firstly this paper investigates systematic approach to automatically recover and match minutiae patterns for the personal identification. Secondly, we also investigate quantification of knuckle minutiae quality recovered from the finger knuckle images and its successful use in more accurately matching the knuckle minutiae. Finally, this paper provides comparative evaluation of three popular minutiae matching approaches, *i.e.*, minutiae cylinder code [9], minutiae triangulation [23] and spectral minutiae matching [13]-[14], for matching of finger knuckle patterns. Our experimental results are presented on finger dorsal image database of 120 subjects and illustrate promises (average rank-one recognition accuracy of 98% to recognize 120 different subjects) from minutiae matching using knuckle patterns. We also provide a tool [24] to analyze minutiae recovery and matching that can be useful, especially for the forensic scientists to recover and analyze minutiae patterns while matching two knuckle patterns. This study detailed in this paper also identifies the need for further research and development of advanced algorithms to more accurately recover/match minutiae patterns from the finger knuckle images.

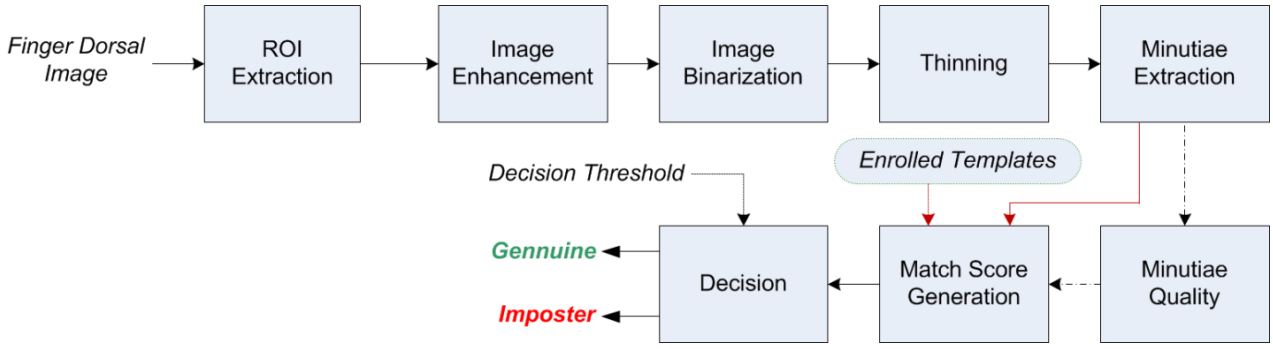

Figure 2: The block diagram illustrating key steps for automatically recovering and matching knuckle minutiae patterns from finger knuckle images.

2. Image Segmentation and Normalization

The block diagram of knuckle minutiae based finger knuckle matching approach investigated in this work is shown in figure 2. Each of the acquired finger dorsal images is almost in vertical pose and additional orientation alignment is not necessary as the minutiae matching methods are least sensitive to the orientation changes. These images firstly subjected to automated segmentation of region of interest (ROI) images that illustrate major knuckle patterns considered in this work. The ROI segmentation strategy

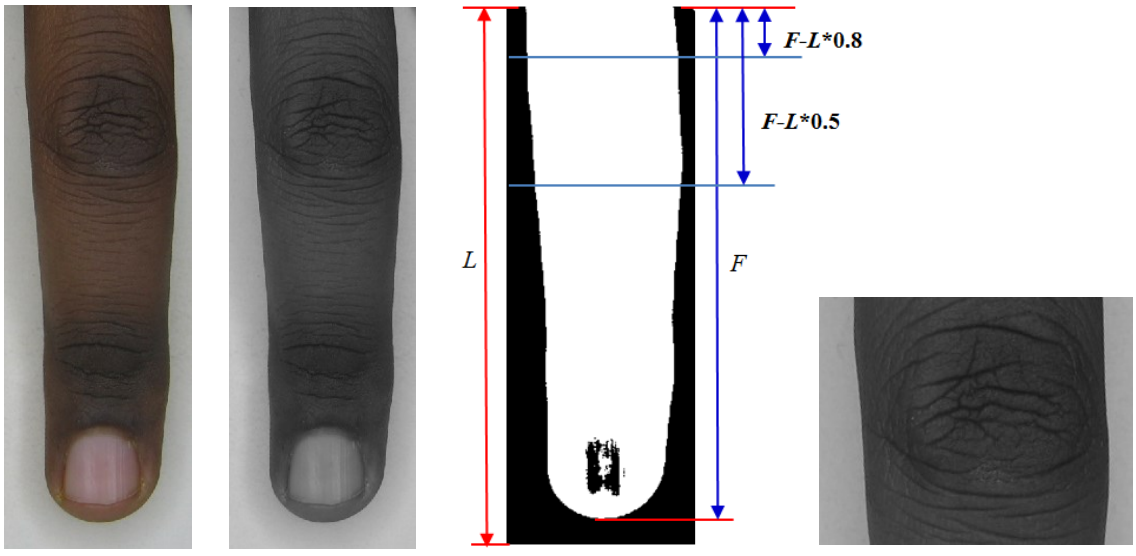

(a) (b) (c) (d)

Figure 3: Extraction of ROI: (a) sample finger dorsal image, corresponding (b) grey level, (c) binarized image and (d) segmented ROI with knuckle patterns.

illustrate major knuckle patterns considered in this work. The ROI segmentation strategy considered in this work is simple and similar as in [8] which can automatically generate normalized and fixed region of interest from finger dorsal images. Each of the images is firstly binarized [11] to generate silhouette representing finger shape (figure 3). The length of finger image (L) and length of finger shape (F) in the silhouette is used to extract the knuckle region image of fixed length which is proportional to the length of the finger. This automatically segmented major knuckle image is used for the image normalization as detailed in the following.

Each of the segmented knuckle image is subjected to image enhancement. Unlike prior methods in the literature for the knuckle enhancement whose objective has been to accentuate contrast of textured in local regions, we explored a variety of image enhancement methods that can enhance contrast for curved lines that form major knuckle patterns. Sample results from the usage of median filter, Butterworth filter (first order

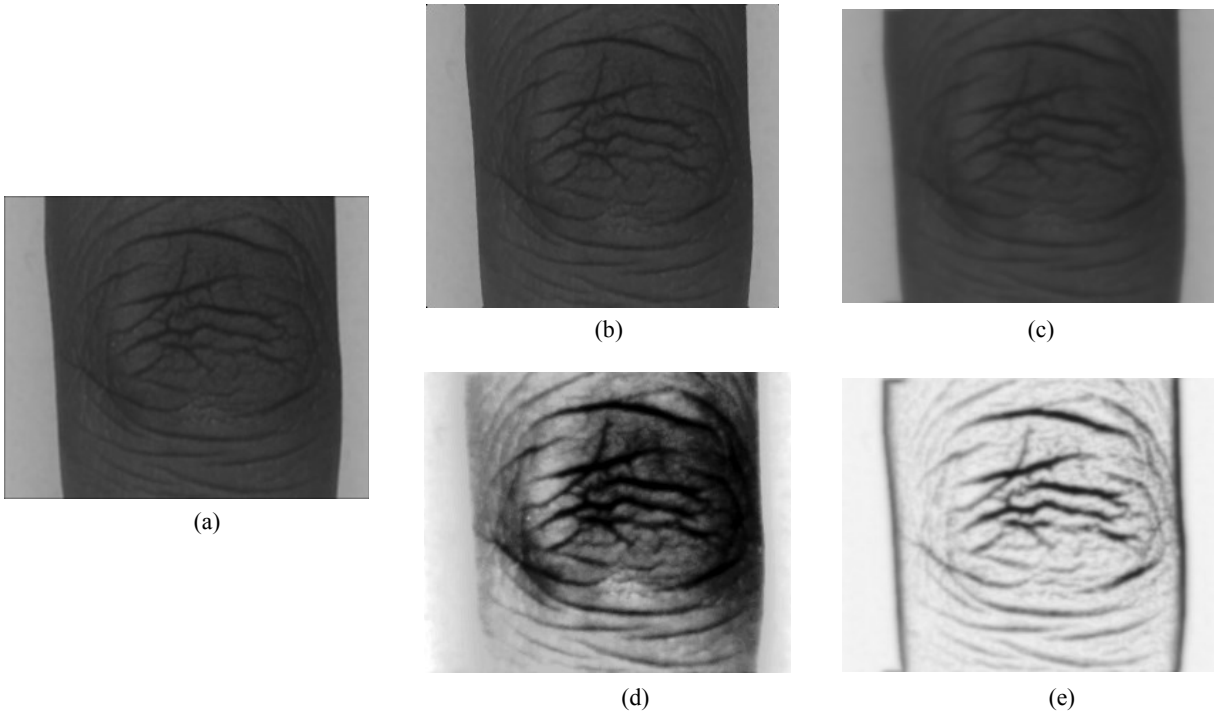

Figure 4: (a) Segmented image, the enhanced image using (b) median filtering, (c) Butterworth filter, (d) histogram equalization, and (e) self-quotient image.

with cutoff frequency of 1/25), histogram equalization and self-quotient image are shown in figure 4.

Each of the segmented knuckle image is firstly subjected to Butterworth filter and then used to generate self-quotient image which is used as enhanced image for further processing. The self-quotient image K_q for knuckle image K, is defined as

$$K_q = \frac{K}{\widetilde{K}} \tag{1}$$

where $\widetilde{K}$ is the filtered image using anisotropic filters as detailed in [10], [25]. The self-quotient knuckle image can significantly help to enhance the contrast for major curved lines and also reduce the influence from uneven illumination. Each of the enhanced knuckle images are firstly binarized [11] and the resulting binarized image is subjected to noise removal using dilation and erosion operations (figure 5). The resulting image is

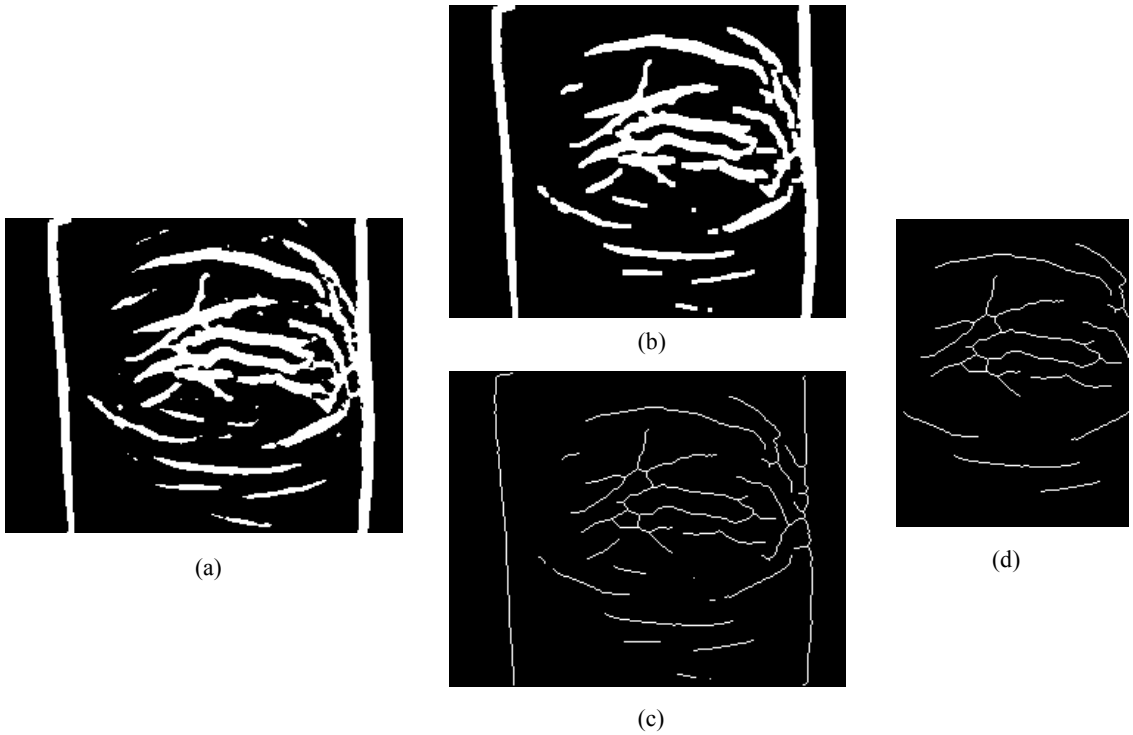

Figure 5: Segmented image after (a) binarization, (b) dilation and erosion, (c) thinning, and (d) after removing isolated noisy pixels.

further subjected to thinning operation and the final region of interest is recovered by eliminating the finger shape boundaries in the thinned images. These edges or shape boundaries are automatically detected by scanning the thinned image, *e.g.* farthest black to white transition among all rows of pixels for the left edges. Isolated noisy pixels are removed from the thinned region of interest image and the resulting (figure 5) image is used to automatically locate the knuckle minutiae as discussed in next section.

3. Minutiae Recovery and Quality Estimation

The thinned region of interest images (figure 5) are used to locate the minutiae features from knuckle patterns. The location and type of minutiae is extracted by using convolving with pre-designed masks that generate specific patterns for the targeted singularities in the thinned image. Such convolution based approach [21] is fast and can accurately localize several categories of minutiae planned to recover in this work. Any kind of minutiae pattern or structure can be detected by this approach which relies on matching of the observed response from the designed mask. Figure 6 illustrates a typical identification of endpoint minutiae from the thinned image using the responses as illustrated below the corresponding minutiae mask. The detection of other kind's minutiae is also similar [13], [21] and was used to identify three types of minutiae, *i.e.*, endpoint, bifurcation and cross points, in our experiments.

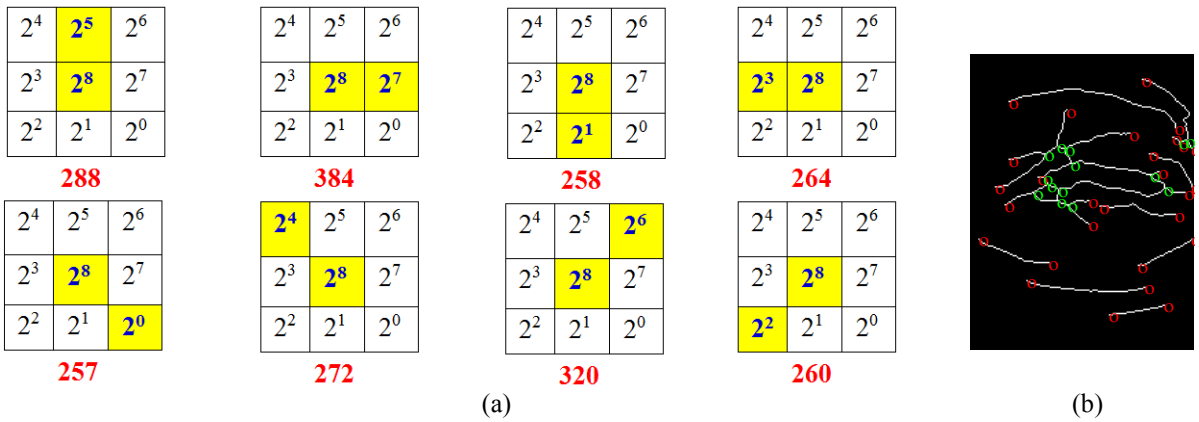

Figure 6: (a) A typical filter response for endpoint minutiae from thinned image and (b) endpoint minutiae (in red circles) and bifurcation minutiae detected from a typical knuckle image.

3.1 Estimating Knuckle Minutiae Quality

Recovery of minutiae from the contactless knuckle images is significantly influenced by the image quality, method of segmentation, finger pose and deformation, image normalization and the method of binarization used to generate thinned images for the minutiae recovery. Therefore the amount of true minutiae recovered, or the proportion of spurious minutiae, recovered from knuckle images can vary from image sample to sample. In fingerprints, the minutiae quality has been successfully investigated to improve the fingerprint matching accuracy. Some references detail computation of fingerprint minutiae quality by measuring their correlation with high quality minutiae image [16] while some compute minutiae quality from the local pixel intensity statistics [5]. In [14], the minutia quality is considered as the minutia reliability and is defined as the probability that a recovered minutia truly exists in physical fingerprints. These methods are suitable for fingerprints or specific matching method. However the finger knuckle patterns do not have regular ridges like the fingerprint and therefore these methods cannot work well for knuckle minutiae. We considered variety of methods to quantify knuckle minutiae and finally employed combination of minutiae quality as described in the following.

3.1.1 Quality using Local Coherence of Gradients

This approach evaluates the gradients of curved knuckle lines corresponding to the foreground area of the recovered minutiae. As detailed in [6], the image quality of the local gradients in the block of size $b \times b$ which is centered at the respective minutiae is extracted. Let $k = (k_x, k_y)$ denote the gradient of the local curves in the background image

block corresponding to the identified minutiae. The covariance matrix from such gradient vectors for all $b*b$ locations in this image block is computed as follows [6]:

$$\Lambda = \frac{1}{b^2}\sum k.k^T = \begin{bmatrix} \lambda_{11} & \lambda_{12} \\ \lambda_{21} & \lambda_{22} \end{bmatrix} \quad (2)$$

The eigenvalues μ_1 and μ_2 from above symmetric matrix are then computed.

$$\mu_1 = \frac{1}{2}(\lambda_{11} + \lambda_{22} + \sqrt{(\lambda_{11} - \lambda_{22})^2 + 4 \times {\lambda_{12}}^2}) \quad (3)$$

$$\mu_2 = \frac{1}{2}(\lambda_{11} + \lambda_{22} - \sqrt{(\lambda_{11} - \lambda_{22})^2 + 4 \times {\lambda_{12}}^2}) \quad (4)$$

The minutiae quality q_i that can represent clarity of local knuckle lines can be computed as follows:

$$q_i = \frac{(\mu_1 - \mu_2)^2}{(\mu_1 + \mu_2)^2} = \frac{(\lambda_{11} - \lambda_{22})^2 + 4 \times {\lambda_{12}}^2}{(\lambda_{11} + \lambda_{22})^2} \quad (5)$$

This quality index in range 0-1 essentially represents the clarity of curved lines in the foreground knuckle patterns.

3.1.2 Quality using Minutiae Localization

The second approach [4] considered in this work is to quantify minutiae quality by considering the distribution of minutiae in neighborhood. Firstly, nearest n minutiae centers around the minutia m_i are located. We then compute the average distance p_i between the neighbor minutiae and the center minutia m_i. The minutiae quality q_g is then computed with by measuring the proximity of neighborhood minutiae as follows:

$$q_g = \begin{cases} 0 & if\ p_i < Pt_1 \\ 1 & if\ p_i > Pt_2 \\ \frac{p_i - Pt_1}{Pt_2 - Pt_1} & otherwise \end{cases} \quad (6)$$

The thresholds Pt_1 and Pt_2 are fixed and empirically determined.

The *combined* knuckle minutiae quality q is generated by weighted combination of two qualities as follows.

$$q = 100 * (\mathrm{w} * q_i + (1 - w) * q_g) \quad (7)$$

The quality of every knuckle minutiae is therefore quantified in the range of 0-100. The parameter w is empirically determined to generate best performance (lower equal error rate) and kept as 0.7 for all experiments in this paper. The minutiae quality is used to improve the matching accuracy of knuckle minutiae as described in section 4.

3.1.3 Evaluating Quality of Knuckle Minutiae

Unlike fingerprint ridges, the thickness of knuckle curves and lines varies along the curved profile. Therefore it is judicious to ascertain minutiae quality by varying block size b in corresponding knuckle image. In all our experiments detailed in this paper the parameters for quality evaluation are fixed as $n = 3$, $Pt_1 = 3$, and $Pt_2 = 15$. Figure 7

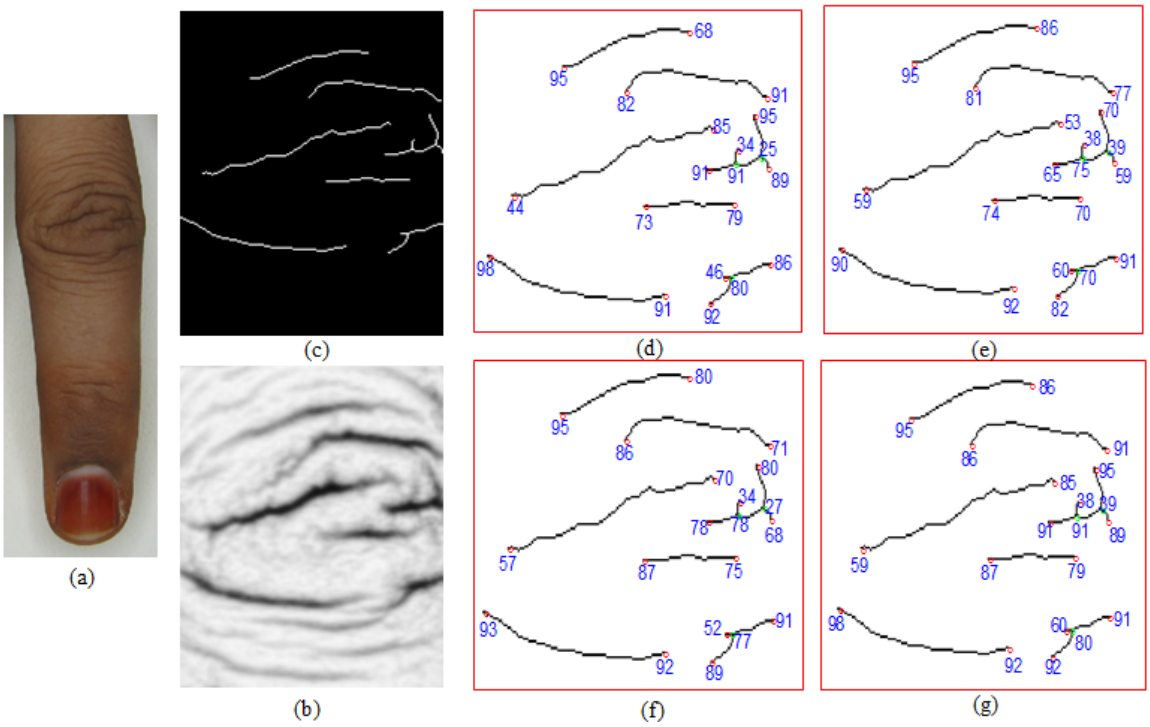

Figure 7: (a) Sample finger dorsal image, (b) segmented and enhanced image, (c) thinned image, (d) minutiae quality with b = 5, (e) b = 9, (f) b = 13, and with (g) maximum of quality from (d)-(f).

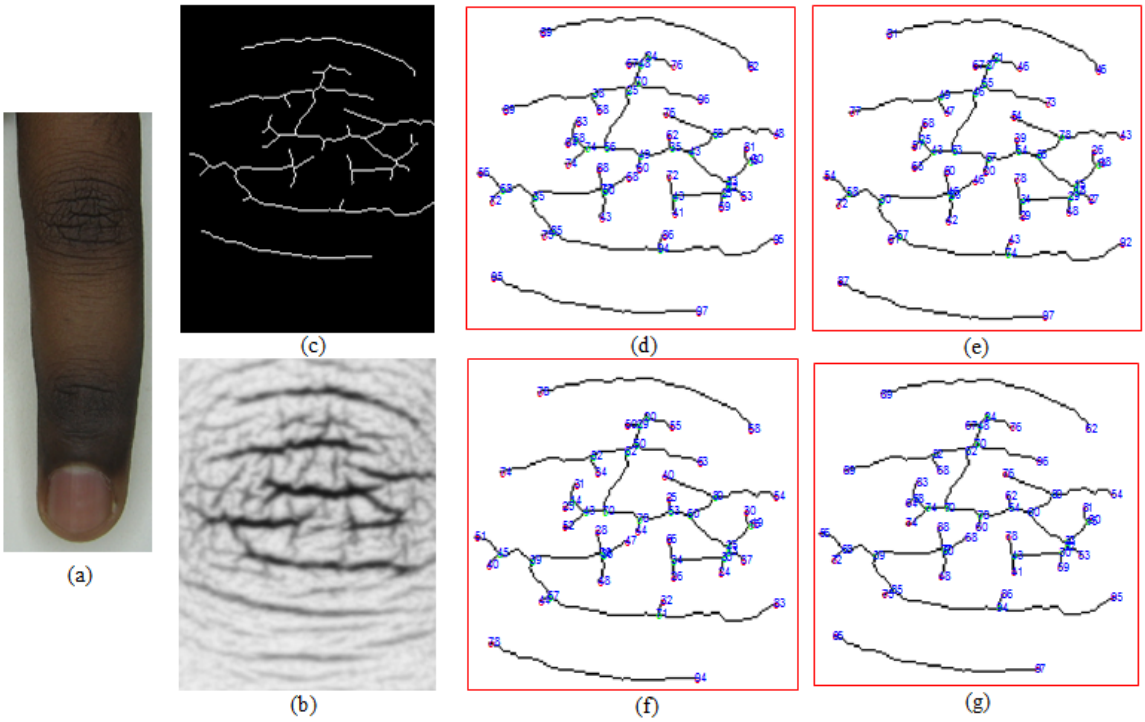

Figure 8: (a) Sample finger dorsal image, (b) segmented and enhanced image, (c) thinned image, (d) minutiae quality with b = 5, (e) b = 9, (f) b = 13, and with (g) maximum of quality from (d)-(f).

illustrates the knuckle minutiae quality from a typical finger knuckle image using different block sizes b. This figure shows knuckle minutiae quality obtained with 5 × 5 (figure 7d), 9 × 9 (figure 7e) and 13 × 13 (figure 7f). Figure 7(g) illustrates knuckle minutiae quality obtained by maximum of minutiae quality obtained by varying block sizes in Figure 7(d)-(f) and is employed in further experiments detailed in section 4,1 and 4.3. Figure 8 illustrate another sample knuckle image and similar computation of knuckle minutiae quality as in figure 7. The knuckle minutiae appearing on clearer curves have better quality while their smaller distance with neighboring minutiae reduces the quality score.

4. Matching Knuckle Minutiae

There are a wide variety of approaches developed to match fingerprint minutiae that can be explored for matching the knuckle minutiae. In this work, we considered three approaches to match the recovered knuckle minutiae and are briefly discussed in the following.

4.1 Minutiae Triangulation

This approach considers unique topological structure of neighboring minutiae using the Delaunay triangulation. A typical knuckle minutiae can be represented by its location, curve orientation, and the quality as $m = (x, y, \theta, q)$. The length and orientation of three edges of triangles formed by the minutiae is separately computed. Similar to as in [12], we consider four types of such triplets resulting from types of knuckle minutiae combination as summarized in the following:

Table 1: Classification of knuckle minutiae triplets.

Triplet Type	*Minutiae Type*		
I	*e*	*e*	*e*
II	*e*	*e*	*c*
III	*e*	*c*	*c*
IV	*c*	*c*	*c*

e – Ending, *c* – Bifurcation or Cross

The matching of same types of triplets is achieved as follows:

$$(d_1, d_2) \triangleq \left(\frac{l_1}{l_3}, \frac{l_2}{l_3}\right), \quad l_1 \le l_2 \le l_3, \quad (\cos\theta_1, cos\theta_2, cos\theta_3) \quad (8)$$
$$(\cos\phi_1, cos\phi_2, cos\phi_3) \qquad \phi_1 \le \phi_2 \le \phi_3$$

where l_1, l_2, l_3 are lengths of three triplet edges, $\theta_1, \theta_2, \theta_3$ are the corresponding orientations, d_1 and d_2 is the normalized length, while ϕ_1, ϕ_2, ϕ_3 represents the orientations of three minutiae. Two triplets considered as being matched if they satisfy the following conditions:

$$|d_1 - d_1'| < T_1, |d_2 - d_2'| < T_1 \quad (9)$$

$$|\cos\theta_1 - \cos\theta_1'| < T_2, |cos\theta_2 - cos\theta_2'| < T_2, |cos\theta_3 - cos\theta_3'| < T_2 \quad (10)$$

$$|\cos\emptyset_1 - \cos\emptyset_1'| < T_3, |cos\emptyset_2 - cos\emptyset_2'| < T_3, |cos\emptyset_3 - cos\emptyset_3'| < T_3 \quad (11)$$

The dash superscript in (9)-(11) represents respective variable for the corresponding to be matched triplet. The decision thresholds T_1, T_2, and T_3 are empirically fixed. The matching score from the two knuckle templates is computed as follows:

$$s_t = \frac{m_m}{m_1 + m_2} \quad (12)$$

where m_m is the number of matched triplets while m_1 is the number of triplets in the first knuckle template and m_2 is the number of triplets in the second template. The triplets match score for different types are assigned a weight and the final match score is generated by combining match scores of different types of triplets as the weighted sum score. If two triangles belong to type I (table 1), we add weight w_1, and we add w_2, w_3, w_4 if two triangles belong to type II, type III, type IV respectively. These weights are fixed as $w_1 = 2$, $w_2 = 4$, $w_3 = 6$, and $w_4 = 8$ for all experiments in this work and are determined from the best combination that generated smallest equal error rate. The thresholds were also empirically fixed as $T_1 = 0.05, \text{and } T_2 = T_3 = 0.1$ for experimental results reported in this paper.

We also performed experiments to evaluate the performance improvement while considering knuckle minutiae quality as discussed in section 3. We firstly compute the match score between two knuckle templates s_t by incorporating all the minutiae to generate triplets as in (12), s_t^{q1}score by using knuckle minutiae with quality greater than 50, and s_t^{q2} score by using knuckle minutiae with quality greater than 70. In all our experimental results reported in this paper, more importance is given to match scores generated from triplets with higher quality knuckle minutiae, and final quality based match score is computed using weighted combination as follows.

$$s = (0.2 * s_t) + (0.3 * s_t^{q1}) + (0.5 * s_t^{q2}) \quad (13)$$

4.2 Minutiae Cylinder-Code

This minutiae cylinder-code described in [9] is a fixed-length minutiae based descriptor which is computationally simple and has shown to offer higher accuracy than well-known minutiae based local matching techniques developed for the fingerprints. This approach considers distance of one minutia to its neighboring minutiae and is the basis of this descriptor. The minutiae cylinder-code (MCC) [9] encodes each of the minutiae into a discretized 3D cylinder-shaped structure which can also encode angular distances. Therefore MCC based matching of knuckle minutiae templates was also evaluated in our experiments.

4.3 Spectral Minutiae

The spectral minutiae approach is detailed in [13]-[14] and has shown to offer accurate matching for the fingerprint and vascular minutiae templates. Therefore this scheme was also investigated for the match performance using knuckle minutiae templates. The spatial location (x_i, y_i) and orientation θ_i of each of the knuckle minutiae is firstly used to represent corresponding Gaussian function with variance σ. These set of functions are combined to generate a spatial function $g(x, y)$ whose Fourier transform G computed to generate following spectral function.

$$G = |\exp(-\frac{{\omega_x}^2+{\omega_y}^2}{2\sigma^{-2}}) \times \sum_1^z \exp\left(-j\left(\omega_x x_i + \omega_y y_i\right) + j\theta_i\right)| \qquad (14)$$

The magnitude of the Fourier spectrum in above function can ensure that this representation is invariant to translation and rotation of the templates. This spectral representation G is sampled on a on a polar-logarithmic grid to obtain spectral minutiae representation. Figure 9 illustrates such representation of knuckle minutiae templates from a sample in the database. In all our experiments, we use $M = 128$ samples between 0.1 and 0.6 in the radial direction. In the angular direction, we employed $N = 256$ samples uniformly distributed between 0 and 2*pi. Let $G_1(m, n)$ and $G_2(m, n)$ represent two minutiae spectra in the polar-logarithmic domain for the two knuckle minutiae templates

being matched. The match score s_g between two such knuckle templates is computed as follows:

$$s_g = \frac{1}{MN}\sum_{m=1,n=1}^{M,N} \tilde{G}_1(m,n)\tilde{G}_2(m,n) \quad (15)$$

where $\tilde{G}_1(m,n)$, $\tilde{G}_2(m,n)$ respectively represents $M \times N$ size normalized $G_1(m,n)$, $G_2(m,n)$ with zero mean and unit energy. We also performed experiments to evaluate spectral minutiae matching using knuckle minutiae quality. In all such experiments, the knuckle minutiae with quality less than 50 are removed and the match score is only computed from rest of the knuckle minutiae.

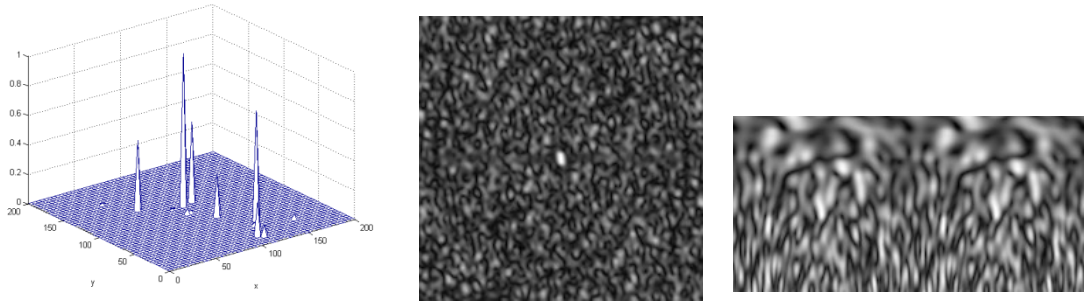

(a) (b) (c)

Figure 9: Spectral knuckle minutiae representation: (a) representation of knuckle minutiae points, from a sample knuckle template, as a set of isotropic 2D Gaussian functions, (b) its Fourier spectrum and (c) sampled Fourier spectrum on a polar-logarithmic grid.

5. Experimental Results

Our key objective in this work has been to evaluate the recovery and matching of minutiae features from the finger knuckle images. We used an extended version of finger dorsal image database in [8] for the performance evaluation. This database has five index finger dorsal images each of which are acquired from 120 different subjects. Therefore 600 finger dorsal images are employed to automatically recover major knuckle minutiae templates as discussed in section 2. We were able to recover an average of 13.85 end points per knuckle image (minimum of 4 while maximum of 35) from 600 knuckle images employed in the experiments. The average number of bifurcation minutiae per

knuckle image was 3.97 (minimum of 0 while maximum of 20). The distribution of minutiae quality for different types of minutiae and in their combination is shown in figure 10. It was observed that higher number of endpoint minutiae of higher quality were recovered (or assigned) while high quality bifurcation minutiae recovered are smaller.

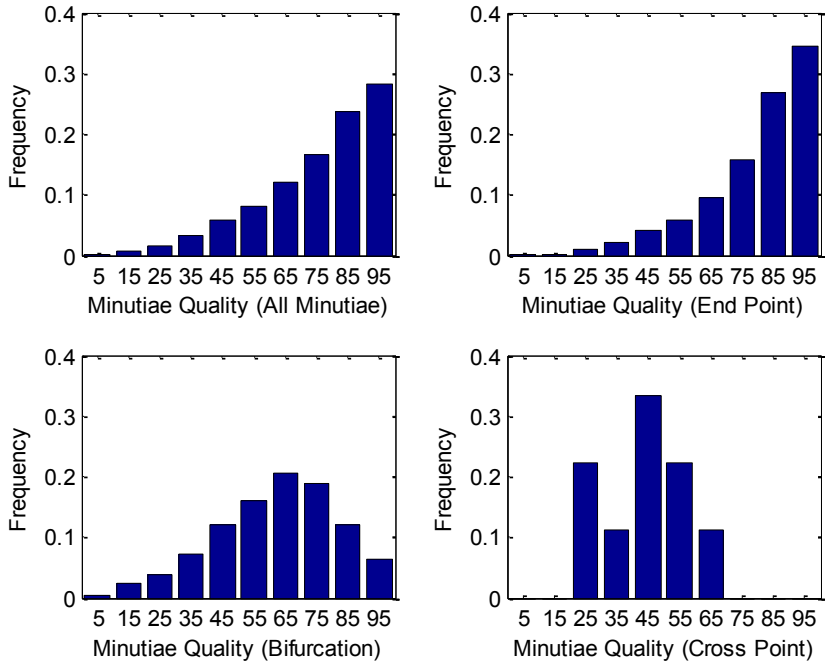

Figure 10: Distribution of knuckle minutiae quality from the minutiae recovered using 600 knuckle images.

The knuckle minutiae experiments were performed using two different protocols. The first protocol, referred as protocol A, uses all the combination of matches between two knuckle images and generates 1200 (10 × 120) genuine and 357,000 (5 × 5 × 119 × 120) impostor scores using all-to-all approach [15]. The second protocol, referred here as protocol B, is leave-one-out approach and generates 600 (5 × 120) genuine and 71400 (5 × 119 × 120) impostor match scores. Protocol A was also used to generate or determine parameters cited in different sections earlier.

The receiver operating characteristics (ROC) for knuckle minutiae matching using protocol A is shown in figure 11. This figure also shows the cumulative match characteristics using minutiae matching schemes considered in our experiments. The MCC approach achieves highest EER (table 2) and was therefore not considered for further experimental evaluation. It can be observed from the results in figure 11 that usage of minutiae quality helps to improve the performance. The performance from knuckle minutiae scheme using spectral minutiae is superior.

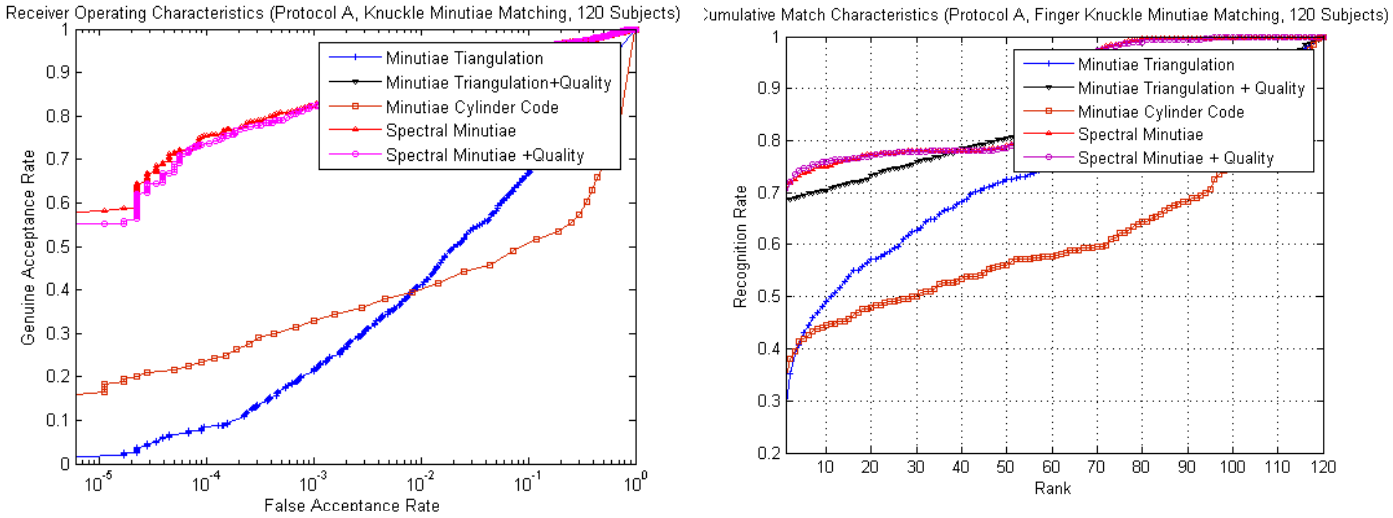

(a) (b)

Figure 11: ROC (a) and CMC (b) using from *protocol A* for matching recovered finger knuckle minutiae using different matching schemes

Table 2: Comparative experimental results from knuckle minutiae matching using protocol A

Minutiae Matching Method	*EER (%)*	*Rank-One Recognition Rate (%)*
Minutiae Triangulation	**21.42**	**28.33**
Minutiae Triangulation + Quality	**11.83**	**66.67**
Minutiae Cylinder Code	**37.08**	**34.17**
Spectral Minutiae	**6.33**	**70.5**
Spectral Minutiae + Quality	**5.58**	**69.67**

The ROC for knuckle minutiae matching using protocol B is shown in figure 12. This figure also shows the CMC using protocol B for the corresponding minutiae matching

schemes. Table 3 summarized the equal error rate (EER) and the rank-one recognition accuracy from the experiments using protocol B. It can be observed from the results that spectral minutiae approach offers superior matching accuracy and use of minutiae quality can also help for improving the minutiae matching accuracy. The experimental results presented in figure 11-12 are promising and validate the success of recovering and matching the minutiae from the finger knuckle images. Figure 13 illustrates the graphical

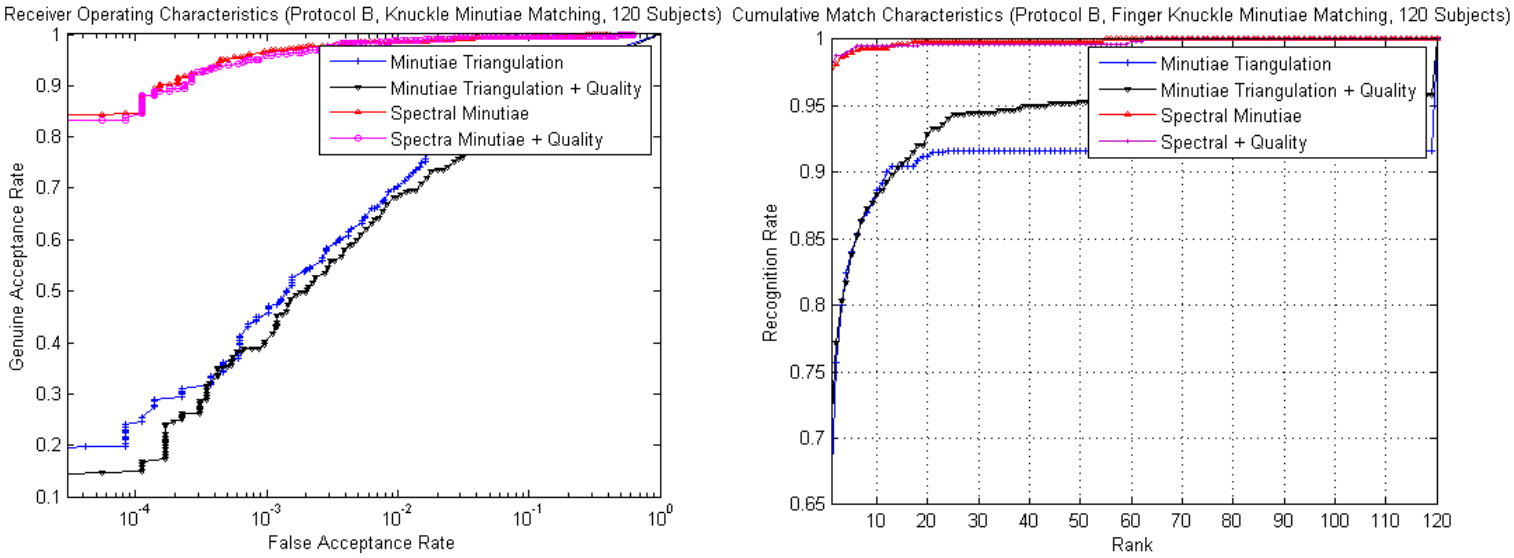

(a) (b)

Figure 12: ROC (a) and CMC (b) using from *protocol B* for matching recovered finger knuckle minutiae using different matching schemes.

Table 3: Comparative experimental results from knuckle minutiae matching using protocol B.

Minutiae Matching Method	*EER (%)*	*Rank-One Recognition Rate (%)*
Minutiae Triangulation	**9.33**	**66**
Minutiae Triangulation + Quality	**11.67**	**70.83**
Spectral Minutiae	**1.5**	**97.5**
Spectral Minutiae + Quality	**1.17**	**98**

presented in figure 11-12 are promising and validate the success of recovering and matching the minutiae from the finger knuckle images. Figure 13 illustrates the graphical user interface developed to analyze and match the minutiae from the finger knuckle

images. This tool is made available via [24] and can be helpful in recovering and matching minutiae patterns from knuckle images, especially for the forensic applications.

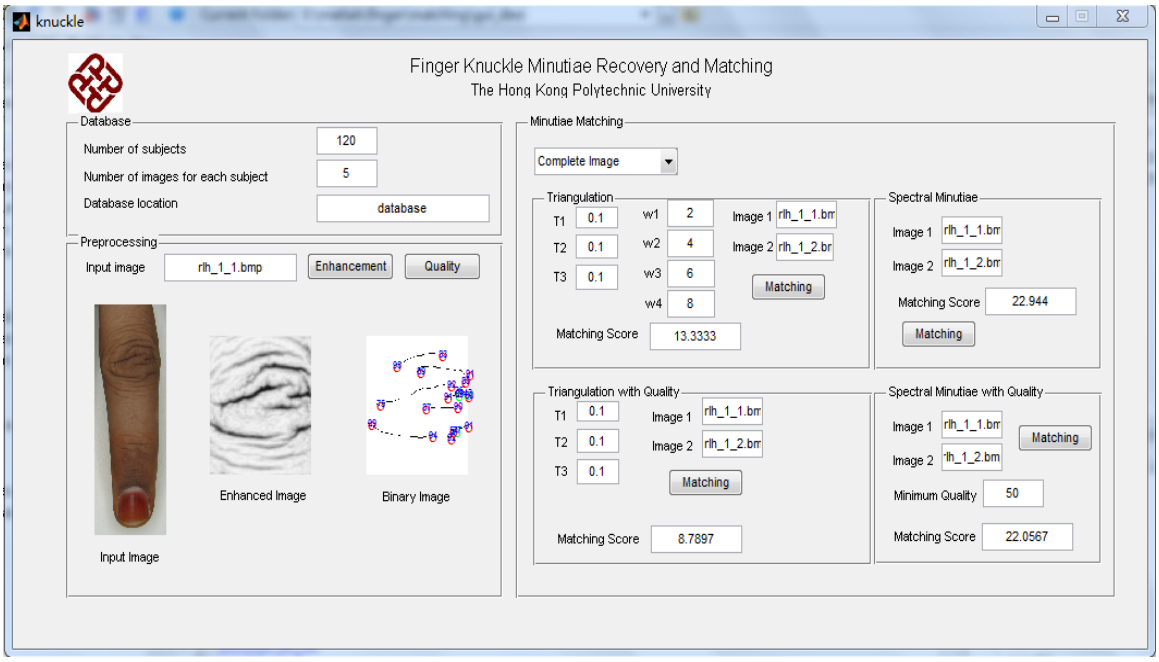

Figure 13: Interface for tool to recover/match minutiae from knuckle images.

6. Conclusions and Further Work

This paper has presented the first attempt to recover and match finger knuckle minutiae for the biometric identification. The study performed in this paper is motivated for the possible use of knuckle patterns for forensic analysis and is based on popularity of minutiae matching approach for prosecution of suspects from the forensic analysis. Our efforts detailed in this paper to automatically recovery of finger knuckle minutiae and the quantification of knuckle minutiae quality has been quite successful as it has been able to achieve promising matching accuracy. It was observed that the performance from the minutiae triangulation approach was quite poor while the spectral matching of knuckle minutiae delivered the best performance. The poor performance from the minutiae triangulation can be attributed to the sensitivity of this approach to the missed or spurious

minutiae. If some minutiae are missed after the preprocessing of knuckle images the structure of the actual triplets can be significantly different. The spectral minutiae approach on the other hand is more tolerant to the alignment/registration of minutiae between two templates as it represents minutiae templates in a translation invariant spectrum, in which the rotation and scaling results in translations which are easier to be accommodated during the matching.

Despite the first promising effort to investigate recovery and matching of knuckle minutiae, there are some open issues that should be addressed to achieve more reliable recovery and accurate matching of knuckle minutiae. The discontinuity of knuckle curve can result in spurious minutiae which degrades the matching accuracy. Unlike fingerprint ridges, the knuckle curves are irregular and often vary in thickness. Some curves are lost during the preprocessing, largely due to the adverse effect of illumination, pose and rotation in the contactless finger knuckle images. Therefore more effective approach to recover irregular curves and quantify knuckle minutiae quality should be developed in further extension of this work. Although more work remains to be done, our investigation presented in this paper constitute a promising addition to biometrics security, especially for forensic applications when knuckle patterns from suspects can be retrieved from image data.

References

[1] *Strengthening Forensic Science in the United States: A Path Forward,* National Research Council, National Academic Press, Washington DC, USA, 2009.

[2] D. L. Woodard and P. J. Flynn, "Finger surface as a biometric identifier", *Computer Vision and Image Understanding*, vol. 100, no. 3, pp. 357-384, Dec. 2005.

[3] G. S. Morrison, "Distinguishing between forensic science and forensic pseudoscience: Testing of validity and reliability, and approaches to forensic voice comparison," *Science & Justice*, vol. 54, pp. 245-256, 2014.

[4] K. Cao, E. Liu, L. Pang, J. Liang, and J. Tian, "Fingerprint matching by incorporating minutiae discriminability," *Proc. IJCB 2011*, pp. 1-6, Washington DC, 2011.

[5] D.-H. Kim. "Minutiae quality scoring and filtering using a neighboring ridge structural analysis on a thinned fingerprint image," *Proc. AVBPA 2005*, pp. 674–682, Jul. 2005.

[6] Y. Chen, S. Dass, and A. Jain, "Fingerprint quality indices for predicting authentication performance," *Proc. ABVPA 2005*, LNCS 3546, pp. 160-170, 2005.

[7] Bromley Paedophile Dean Hardy Jailed for 10 Years, *Bromley Times*, January 2012. http://www.bromleytimes.co.uk/news/court-crime/bromley_paedophile_dean_hardy_jailed_for_10_years_1_1176957
[8] A. Kumar and Ch. Ravikanth, "Personal authentication using finger knuckle surface", *IEEE Trans. Info. Forensics & Security*, vol. 4, no. 1, pp. 98-110, Mar. 2009.
[9] R. Cappelli, M. Ferrara, and D. Maltoni. "Minutia Cylinder- Code: A New representation and matching technique for fingerprint recognition," *IEEE Trans. Pattern Anal. & Machine Intell.*, vol. 32, pp. 2128–2141, Dec. 2010.
[10] H. Wang, S. Z. Li. and Y. Wang, "Face recognition under varying lighting conditions using self-quotient image," *Proc. FG 2004*, pp. 819-824, 2004.
[11] N. Otsu, "A threshold selection method from gray-level histograms," *IEEE Trans. Systems, Man and Cybernetics*, vol. 9, pp. 62-66, 1979.
[12] A. Kumar and K. V. Prathyusha, "Personal authentication using hand vein triangulation and knuckle shape," *IEEE Trans. Image Process*., vol. 18, pp. 2127–2136, 2009.
[13] D. Hartung, M. A. Olsen, H. Xu, H. T. Nguyen, C. Busch, "Comprehensive analysis of spectral minutiae for vein pattern recognition," *IET Biometrics*, pp. 25–36, 2012.
[14] H. Xu and R. Veldhuis, "Spectral minutiae representations of fingerprints enhanced by quality data" *Proc. BTAS*, Washington DC, Sep. 2009.
[15] T.-S. Chan and A. Kumar, "Reliable ear identification using 2D quadrature filters," *Pattern Recognition Letters*, vol. 33, issue 14, pp. 1870-1881, 2012.
[16] F. Chen and Y.-S. Moon, "Fingerprint matching with minutiae quality score," *Proc. ICB 2007*, LNCS 4642, pp. 663–672. 2007.
[17] A. K. Sricharan, A. Reddy and A. G. Ramakrishnan, "Knuckle based hand correlation for user verification," *Proc. SPIE*, vol. 6202, *Biometric Technology for Human Identification* III, P. J. Flynn, S. Pankanti (*Eds*.), 2006.
[18] L. Zhang, L. Zhang, D. Zhang and H. Zhu, "Online finger-knuckle-print verification for personal authentication," *Pattern Recognition*, vol. 43, no. 7, pp. 2560-2571, Jul. 2010.
[19] A. Kumar and Y. Zhou, "Human identification using knucklecodes," *Proc. BTAS 2009,* Washington DC, pp. 147-152, Sep. 2009.
[20] K. Y. Cheng and A. Kumar, "Contactless finger knuckle identification using smartphones," *Proc. BIOSIG 2012,* Darmstadt, Sep. 2012.
[21] M. A. Olsen, D. Hartung, C. Busch, R. Larsen, "Convolution approach for feature detection in topological skeletons obtained from vascular patterns" *Proc. IEEE Sym. Computational Intelligence* Apr. 2011.
[22] A. Kumar, "Can we use minor finger knuckle images to identify humans?," *Proc. BTAS 2012*, pp. 55-60, Washington DC, Sep. 2012.
[23] T. Uz, G. Bebis, A. Erol, S. Prabhakar, "Minutiae-based template synthesis and matching for fingerprint authentication," *Computer Vis. & Image Understanding*, pp. 979-992, vol. 113, 2009.
[24] Weblink to download GUI based analysis tool for Knuckle Minutiae Patterns, http://www.comp.polyu.edu.hk/~csajaykr/Knuckle_Minutiae.rar
[25] V. Ttruc, N. Pavei, "Photometric normalization techniques for illumination invariance, in: Y.J. Zhang (*Ed*), Advances in Face Image Analysis: Techniques and Technologies, IGI Global, pp. 279-300, 2011.